

# Facial Surgery Preview Based on the Orthognathic Treatment Prediction

Huijun Han<sup>a,e</sup>, Congyi Zhang<sup>b</sup>, Lifeng Zhu<sup>c</sup>, Pradeep Singh<sup>a</sup>, Richard Tai-Chiu Hsung<sup>d</sup>, Yiu Yan Leung<sup>d,1</sup>, Taku Komura<sup>b</sup>, Wenping Wang<sup>e</sup>, Min Gu<sup>a,\*</sup>

<sup>a</sup>*the Discipline of Orthodontics, Faculty of Dentistry, the University of Hong Kong, Hong Kong SAR, China*

<sup>b</sup>*the Department of Computer Science, Faculty of Engineering, The University of Hong Kong, Hong Kong SAR, China*

<sup>c</sup>*School of Instrument Science and Engineering, Southeast University, Nanjing, China*

<sup>d</sup>*the Discipline of Oral and Maxillofacial Surgery, the University of Hong Kong, Hong Kong SAR, China*

<sup>e</sup>*the Department of Computer Science and Engineering, Texas A&M University, Texas, USA*

---

## Abstract

Orthognathic surgery consultation is essential to help patients understand the changes to their facial appearance after surgery. However, current visualization methods are often inefficient and inaccurate due to limited pre- and post-treatment data and the complexity of the treatment. To overcome these challenges, this study aims to develop a fully automated pipeline that generates accurate and efficient 3D previews of postsurgical facial appearances for patients with orthognathic treatment without requiring additional medical images. The study introduces novel aesthetic losses, such as mouth-convexity and asymmetry losses, to improve the accuracy of facial surgery prediction. Additionally, it proposes a specialized parametric model for 3D reconstruction of the patient, medical-related losses to guide latent code prediction network optimization, and a data augmentation scheme to address insufficient data. The study additionally employs FLAME, a parametric model, to enhance the quality of facial appearance previews by extracting facial latent codes and establishing dense correspondences between pre- and post-surgery geometries. Quantitative comparisons showed the algorithm's effectiveness, and qualitative results highlighted accurate facial contour and detail predictions. A user study confirmed that doctors and the public could not distinguish between machine learning predictions and actual postoperative results. This study aims to offer a practical, effective solution for orthognathic surgery consultations, benefiting doctors and patients.

*Keywords:* Computer-aided detection and diagnosis, geometric deep learning, visualization

---

## 1. Introduction

Orthognathic surgery corrects facial asymmetry and abnormalities, improving aesthetics, oral function, and psychosocial well-being. However, patients often feel anxious due to uncertainty about their post-surgical appearance, impacting communication with their doctors. Providing accurate previews of the expected outcome can help reduce pre-surgical anxiety, set realistic expectations, and increase patient satisfaction.

While Virtual Surgical Planning (VSP) tools (e.g. Dolphin [10], Morpheus 3D FaceMaker[4], and 3dMD Vultus [1]) provide clinical level high accuracy results for surgery planning use, they require Computed Tomography (CT) or Cone Beam Computed Tomography (CBCT) imaging data as additional inputs, which is always inaccessible for preview purpose. The introduction of CT/CBCT data has some practical limitations: It significantly increases the requirements of capturing data for users in search of functional or aesthetic improvements for jaws. On the other hand, due to the complexity of clinical simulations, this

type of tools requires significant expertise and labor from physicians and cannot be fully automated. Therefore, the series of surgical planning tools cannot be used as preview tools for the general public.

Several machine learning-based solutions have been proposed for facial surgery preview purposes. These solutions utilize dense multilayer perceptrons (MLP) [25, 26, 3, 23, 20], or employ a conditional generative adversarial network [21, 13] to predict 3D coordinate changes. However, these solutions require X-ray or CT data and target positions of anatomical landmarks as additional input, which can only be specified by clinicians, making them not fully automated. Furthermore, the use of surgical planning parameters by medical professionals significantly increases the cost and complexity of these approaches. As a result, they may not be feasible for individuals seeking quick and intuitive surgical consultations. Currently, available clinician-oriented solutions only provide automated diagnosis and treatment simulations for clinical and research purposes, and there is no study focusing on automatic facial surgery preview specifically for patient visualization purposes.

A patient-oriented solution for visualizing surgical outcomes should be more accessible than a professional doctor-oriented one. In the early consultation stage, po-

---

\*corresponding author

Email address: drgumin@hku.hk (Min Gu)

tential patients are not obligated to take CBCT or X-ray imaging, which would expose users to radiation. Instead, 3D facial reconstruction (e.g., 3dMD (3dMD Inc., Atlanta, GA, USA), Bellus3D (Bellus3D Inc., Los Gatos, CA, USA), and Ein-Scan3D (Shining 3D Technology, Hangzhou, China)) is much safer for post-treatment preview purpose. The solution should be fully automatic and efficient, providing prompt visualization to the user. An automatic facial surgery preview can serve as an effective educational and motivational tool for patients, in addition to serving as a visual aid in acceptance of the treatment.

Our algorithm is designed to predict 3D post-surgery facial appearance based on preoperative facial scans of patients without the need for additional medical images (e.g., X-Ray or CBCT). To address the challenge posed by insufficient data, we develop a data augmentation method that substantially amplifies the available dataset for orthognathic treatment. To explicitly encode the assessment rule in orthognathic treatment, we introduce two medical losses, mouth-convexity loss and asymmetry loss, consistent with surgical definitions that help achieve the optimization goals of surgery. Moreover, our algorithm leverages the unique capabilities of FLAME [15, 30, 16], a parametric model, to extract facial features and build dense correspondences between pre- and post- facial geometries, which is crucial for texture transfer.

In summary, our **contributions** are: (1) We introduce two novel losses: mouth-convexity loss, and asymmetry loss, that align with the goal of orthognathic surgery, to improve prediction accuracy; (2) We propose an effective data augmentation scheme addressing the prevalent issue of insufficient data in medical practice; (3) We complete a fully automated pipeline that showcases the postoperative changes in facial appearance to patients in 3D.

## 2. Related Work

### 2.1. Virtual Surgery Planning for orthognathic surgery

Using machine learning techniques for surgical prediction has become a popular trend. Data-driven algorithms can be used to estimate the likelihood of surgical necessity and complexity, providing valuable information for surgeons to consider. The study of [11] shows that neural networks can determine the need for orthognathic surgery using only facial photographs. [27] presents a deep learning model to predict the difficulty in extracting teeth using radiographic images. However, these publications were not aiming at only predictions of probability, not predictions in the field of vision.

The researchers have then begun exploring the use of machine learning algorithms to predict facial appearance after surgery. These trials include linear regression [12], multilayer perceptrons [25, 26], and conditional GAN[21]. However, in [26] Rutger’s algorithm did not take into account the significant reduction in facial asymmetry before and after surgery, which may limit its ability to correct

facial asymmetry and predict the appearance of asymmetric patients accurately, as Rutger acknowledged. In [25], Tanikawa’s network, trained on fewer than 100 patients, predicts postoperative displacement of dense point coordinates. However, the high dimensionality of the input and output layers (around 18,000) raises overfitting concerns. In addition, part of the network input is derived from CBCT data, which are difficult to obtain as previously mentioned. In [21], while cGAN has proven effective in predicting changes in facial appearance after orthodontic surgery, its applicability to predicting changes after orthognathic surgery may be limited. This is because orthognathic surgery involves greater complexity and a wider range of factors to consider compared to orthodontic surgery. [18] proposes a deep learning framework, FC-Net, the first deep learning-based method to predict postoperative facial changes in patients with skull-facial deformities. Its main purpose is for the doctors to use, as during the inference stage, the precise location of bone movement must be provided by the doctor as a reference in order to present the postoperative appearance.

### 2.2. Facial beautification

**2D Beautification Techniques.** While there are numerous recreational facial beautification applications, they are not suitable for presenting post-surgical results to patients due to their lack of medical foundation and surgical background. Most of these software are based on one-click beautification techniques that reflect popular aesthetics and do not allow fine manipulation by surgeons. Furthermore, the effects of commercial applications such as B612 [7], ModiFace [5], and YouCam [6] can exceed what can be achieved by orthognathic surgery. In contrast, our proposed algorithm is based on the displacement of vertices and can precisely beautify facial contour in a medically sound manner. 2D facial enhancement can also be achieved by using face-swap methods. FaceShifter [14], a two-stage framework that uses innovative encoding and refinement techniques to swap faces, is capable of facial beautification while preserving identity. FSGAN[19] presents a subject-agnostic face swapping and reenactment approach that does not require training on specific face pairs, featuring a novel iterative deep learning method for handling significant pose and expression variations. The subject-agnostic nature of the method makes it more accessible and user-friendly for people seeking medical consultation, since they do not need to provide training data for each pair of faces they want to swap or re-enact.

**3D Beautification Techniques.** 3D beautification can be achieved through 3D facial reconstruction, which has evolved from large-scale modeling (LSFM in [2]) to capturing details and customizing for specific individuals or groups, enhancing the overall visual appeal and aesthetics of the reconstructed face. In [17], the Structure-Aware Editable Morphable Model (SEMM) introduces a detailed structure representation, addressing the need to capture

facial details in addition to overall geometry. SEMM provides detailed facial representation and intuitive wrinkle manipulation, enabling precise age-related feature control for realistic facial beautification. Detailed reconstructions are highly beneficial for predicting outcomes in medical aesthetics and plastic surgery, allowing more accurate and effective treatment planning. In terms of orthognathic surgery, Qiu proposed SCULPTOR in [22], a skeleton-consistent face generator that can predict facial changes consistent with skeletal variations, especially those resulting from dental surgery. Sculptor, as a refined 3DMM specifically designed for orthognathic surgery, could provide more effective predictions for virtual surgery planning if it were open source, benefiting practitioners and patients by improving surgical outcomes.

### 3. Methodology

We present a simple and effective pipeline to predict 3D face models after surgery, as shown in Fig.1. With a reconstructed 3D facial model as input, we encode it as a latent code with the help of FLAME [15], a parametric facial model. Then we adopt a face predictor to predict the difference between the post- and pre- surgery faces under our well-tailored losses. Those losses not only consider the deviation between latent codes, but also explicitly formulate the facial-asymmetry and mouth-convexity rules of aesthetics in the orthognathic field. Those rules are computed on the predicted facial geometry directly and back-propagated to the network in a differentiable manner. Finally, owing to the mesh coherence in the FLAME model, as a better visualization, we transfer the texture from pre-treatment 3D facial scans to our predicted face models to provide a fully textured post-treatment preview.

As we discussed earlier, to address the challenge of insufficient training data, we also propose a novel data augmentation approach to significantly increase the number of face pairs.

This study was conducted with the approval of the Institutional Review Board (IRB) under the joint agreement of the University of Hong Kong and Hospital Authority Hong Kong West Cluster. The IRB reference number for this study is UW 21-140, with approval granted on February 17, 2021. All procedures adhered to the Declaration of Helsinki and local regulatory requirements.

#### 3.1. Prediction Network

We adopt a predictor and its associated losses for the prediction of facial appearance of orthognathic surgery, as shown in Fig. 1. As a parameterized and differentiable facial model, FLAME can serve as both a pre-trained encoder, compressing geometric information into a latent code, and also a decoder layer, providing the necessary geometric information in a differentiable manner for explicit supervision, which helps update the parameters in the code difference predictor.

The overall loss function used in our algorithm is composed of four components: the mouth convexity loss, the asymmetry loss, the latent code loss, and the geometry loss.

The main challenge in training the predictor comes from the imperfect training data. Our training data consist of real orthognathic surgery cases. However, due to some practical limitations or customized considerations, the post-treatment facial appearance may not be ideal from a clinical perspective, e.g. some of them are still asymmetric or protruding to a certain extent. Adopting a pure data-driven loss in supervision would yield the same artifacts as observed in the training data. To this end, we formulate two explicit clinical rules as our novel losses, the mouth-convexity loss and the asymmetry loss, to enhance the functional and aesthetic aspects.

**Mouth-convexity loss:** *Mouth convexity* refers to a measurement used in orthognathic surgery to describe the relative position of the mouth, nose, and chin. Mouth convexity helps categorize facial profiles into two main types: convex profiles (where the lower jaw protrudes outward, creating a rounded appearance) and concave profiles (where the lower jaw appears retruded or inwardly curved, resulting in a flatter facial contour).

Orthognathic surgery is a highly effective approach to correcting mouth convexity. By carefully realigning the jawbones, this surgical procedure can significantly improve both the functional and aesthetic aspects of the patient’s facial structure. Therefore, we tailor a specific loss function that penalizes the protruding mouth issues, so as to enable the network to generate more pleased facial geometries.

According to [24], a reference line known as *Steiner-line* (s-line, blue dashed line in Fig.2.a) can be drawn from the middle of the nose base to *pogonion* (the extreme anterior point of the chin) to serve as a basis for assessing the protrusion of the mouth. We denote the distances from the s-line to the midpoints of the upper and lower lips as  $d_u$  and  $d_l$  respectively. Medical standards suggest that lip midpoints within a range of 3 millimeters deviation from the s-line are acceptable. To this end, we devise a mouth convexity loss function  $L(d)$ , where the squared distance is used to penalize cases with mouth convexity.

$$L(d) = \begin{cases} 0, & \text{if } d < 3mm \\ (d - 3)^2, & \text{if } d \geq 3mm \end{cases} \quad (1)$$

Mouth-convexity loss  $L_p$  is the sum of  $L(d_u)$  and  $L(d_l)$ .

**Asymmetry loss:** The degree of chin asymmetry in orthognathic surgery is a major concern, and can be quantified by measuring the symmetry of the chin with respect to the *mid sagittal plane* [8] shown in Fig.2.b, which is the focus of our designed asymmetry loss.

According to the medical definition, we determine the mid-sagittal plane  $S$  (green dashed line in Fig.2.b) by solving a plane that passes through points at the midpoint of the eyebrows and the midpoint of the inner corners of the

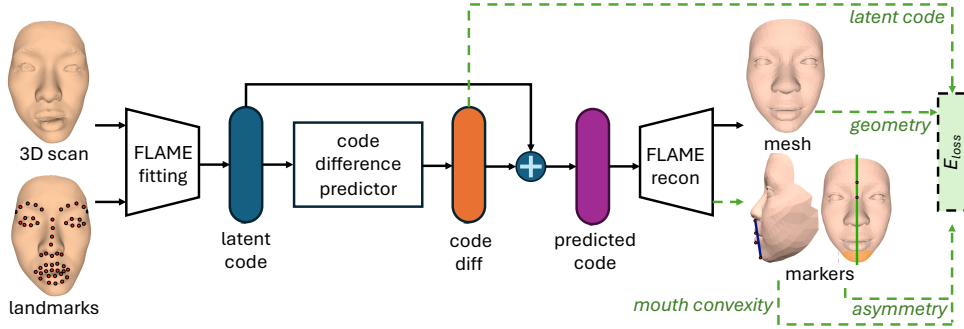


Figure 1: Net architecture for predicting the postoperative appearance from a captured 3D scan. During the training phase, the captured mesh and auto-annotated landmarks are first passed through the FLAME fitting procedure, where they are transformed into a compressed latent code. It is then passed through a predictor and is added into the output code difference. The FLAME reconstructing procedure helps to calculate well-designed losses using markers and mesh. With the help of medical, latent code, and geological types of loss, the parameter of the code difference predictor can be continuously updated. During the testing phase, the data do not flow through the dashed line. The predicted postoperative appearance is generated after FLAME reconstructing.

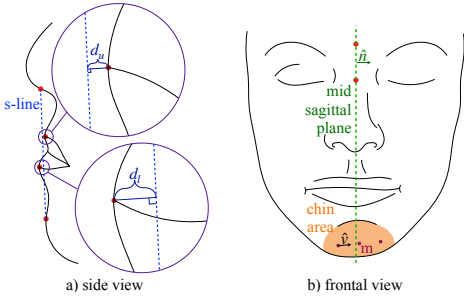


Figure 2: Side view (left) and frontal view (right) of an orthognathic patient for calculating mouth-convexity loss and asymmetry loss respectively.

eyes (red points in Fig.2.b). Because all 3D reconstructed head models of patients are captured with the same natural head position, the ideal unit normal vector  $\hat{n}$  of the mid-sagittal plane is always along the  $x$ -axis. In practice, for each case, we solve the least squares system to determine the mid-sagittal plane  $S$ .

As FLAME uses a topologically symmetric template mesh, we first pair all vertices in the chin area, denoted as  $\{p_i, q_i\}_{i=1, \dots, k}$  (orange region in Fig.2.b). Then we compute the unit direction vectors  $\hat{v}_i$  of the line segments connecting the paired points  $p_i$  and  $q_i$  and their midpoints  $m_i = \frac{1}{2}(p_i + q_i)$ . Following that, we can measure the overall asymmetry of paired points with respect to the mid-sagittal plane using the asymmetry loss

$$L_a = \sum_{i=1}^k d(m_i, S) + (1 - \hat{n} \cdot \hat{v}_i) \quad (2)$$

where  $d(m, S)$  denotes the distance function from point  $m$  to mid-sagittal plane  $S$  and  $\cdot$  is the dot product.

**Latent code loss:** With the aid of a parameterized model serving as an encoder, each pair of preoperative and postoperative captured scans can be encoded as a pair of latent codes. To improve the approximation between the predicted and ground-truth values in the latent space during the training phase, we calculate the squared error

of the latent codes as our latent code loss  $L_f$ :

$$L_f = \|\vec{\beta}_{pred} - \vec{\beta}_{gt}\|_2^2 \quad (3)$$

where  $\|\cdot\|_2$  denotes the  $l^2$  norm,  $\vec{\beta}_{pred}$  and  $\vec{\beta}_{gt}$  are the latent codes of predicted and postoperative GT faces.

**Geometry loss:** The geometry loss  $L_g$  consists of two parts: the point-to-point distance and surface normal errors between the predicted and true meshes:

$$L_g = \frac{1}{N} \sum_{i=1}^N \|p_i^{pred} - p_i^{gt}\|_2^2 + w \frac{1}{M} \sum_{j=1}^M 1 - \cos(\theta_j), \quad (4)$$

where  $N$  and  $M$  are the numbers of points and triangles in the face region,  $p_i^{pred}$  and  $p_i^{gt}$  are the points on the predicted and ground-truth mesh,  $\theta$  is the angle between the predicted and ground-truth surface normal, and  $w$  is the balancing weight.

The geometry part is designed to encourage all the points within our facial mask to be close to their ground-truth values, preventing solely focusing on the chin and mouth areas due to the mouth-convexity loss and asymmetry loss. In addition, the normal part helps the network distinguish between the upper and lower lips, aiding in a better understanding of the facial appearance. We conducted thorough ablation studies in Section 4.4 to verify that geometry loss and latent code loss are not redundant.

**Overall loss function:** we compute the weighted sum of the four losses to form the total loss:

$$L = \alpha_p L_p + \alpha_a L_a + \alpha_f L_f + \alpha_g L_g. \quad (5)$$

### 3.2. Data Augmentation

A sufficient amount of diverse data is essential for updating machine learning model parameters [29], but in orthognathic surgery, data availability is limited by ethical issues and a small number of cases. Additionally, earlier data scarcity was due to the lack of advanced scanning devices, standardized procedures, and insufficient awareness among medical professionals to record 3D facial data. As



a result, data augmentation is vital for predicting orthognathic 3D facial outcomes.

Traditional 3D data augmentation methods like translation, rotation, and scaling may not be effective in our framework without generating meaningful latent codes. Therefore, we propose creating new 3D facial meshes by combining a patient’s lower face with a randomized upper face. The challenge is the difficulty in seamlessly splicing the two due to differences in facial proportions and features. To address this, we design a novel data augmentation algorithm that utilizes FLAME to fit the lower part of postoperative face. Since the fitting process is under-constrained, it enables the generation of multiple outcomes while preserving the same lower face. We perform data augmentation on pairs of pre- and post-surgical scans. For the postoperative side, the data is seamlessly augmented with the synthetic upper face. For the preoperative side, since the surgery only alter the lower face, we stitch the lower part of the preoperative scan with the synthetic upper part to create a seamless model. We also include a data cleaning step to remove outliers caused by the fitting process. By calculating the fitting error of key facial landmarks and setting a threshold, only meshes within the threshold are retained, ensuring the accuracy and reliability of the synthetic meshes.

### 3.3. Integrating FLAME as an encoder-decoder

In our pipeline, FLAME is integrated not only as an encoder to obtain the latent code of captured scans, but also as a decoder to reconstruct facial meshes. As a full-head model with an underlying face skeleton tree composed of neck, jaw, and eyeball joints, FLAME model[15] is defined as:

$$M(\vec{\beta}, \vec{\theta}, \vec{\psi}) = W(T_P(\vec{\beta}, \vec{\theta}, \vec{\psi}), \mathbf{J}(\vec{\beta}), \vec{\theta}, \mathcal{W}), \quad (6)$$

where  $\vec{\beta}$ ,  $\vec{\theta}$  and  $\vec{\psi}$  denote shape, pose and expression vector respectively. During our fitting and reconstruction procedure, the expression vector  $\vec{\psi}$  is not involved, because the patient scanning data were obtained when they were relaxed and in neutral facial expressions and poses.

FLAME, as an encoder, offers better fit accuracy than 3DMM, a linear model based on PCA, due to its incorporation of the jaw joint in its skeleton tree, which captures jaw movements from orthognathic surgeries. As a decoder, FLAME reconstructs facial geometry from the predicted latent code. Geometric information is used to calculate loss during training and optimize the latent code through backpropagation. During inference, the full-face mesh output helps render a textured 3D face model.

### 3.4. Post processing: scan deformation

We aim to provide people who come for surgical consultations with a textured 3D mesh that can be viewed from multiple angles, giving them a comprehensive and visual understanding of their postoperative appearance. To achieve this, we deform the captured facial scan so that it conforms to the predicted FLAME mesh. We morph the

dense grid by deforming the sparse grid. We first build the correspondences between the dense and sparse grids. For each vertex in the dense mesh, we find the closest point in the sparse mesh as its correspondence, whose barycentric coordinate is  $(\lambda_1, \lambda_2, \lambda_3)$  and the morphing displacement of the triangular vertex belonging to it is  $d_1$ ,  $d_2$ , and  $d_3$ . The morphing process is based on the barycentric coordinates, i.e.  $\lambda_1 d_1 + \lambda_2 d_2 + \lambda_3 d_3$ .

## 4. Experiments

### 4.1. Data Collection and Pre-processing

**Data Collection.** Using the 3dMD facial scan acquisition system, 163 pairs of pre- and post-operative 3D facial scans of orthognathic surgery were collected from the University of Hong Kong School of Dentistry. Postoperative scans were taken at least 3 months after the surgical procedure and were used to ensure that the swelling of the patient had subsided and could truly reflect the expected appearance of the patient after surgery. The ratio of male to female patients is 59 : 104, with the majority of Asian patients.

**Data Cleaning.** Our analysis focuses solely on the face, excluding non-facial elements like hair and hats. This ensures that our algorithm can concentrate on key facial areas, such as the chin and nose, while also improving FLAME’s fitting accuracy, as it excludes hair and accessories. To remove non-facial parts, we render the scans from three viewpoints: frontal and both side views with a 45-degree rotation. We then use BiSeNet [28], a bilateral segmentation network, to parse the facial regions from these images, retaining only the relevant areas for analysis.

**Automatic Landmarks annotation.** We used Supervision by Registration [9] with a facial landmark detector to annotate landmarks. A point light was placed in front of the patient’s face to render the mesh to a frontal view image. We then applied a pre-trained landmark detector to extract 2D coordinates for 68 landmarks and transformed them back to 3D using the vertex-to-pixel record. Any drift in landmarks for challenging preoperative cases was manually corrected.

### 4.2. Training details

Our neural network comprises two fully connected modules with a hidden layer of 100 dimensions and input and output layers of 300 dimensions. Additionally, the modules are connected by a batch normalization layer, a nonlinear layer activated by ReLU, and a dropout layer with a 50% probability. The balance parameters  $\alpha_p$ ,  $\alpha_a$ ,  $\alpha_f$ , and  $\alpha_g$  are set to 5000, 5000, 1, and 1 respectively.

During the training process, we set the batch size to 150, and trained our model for a total of 500 epochs. The original learning rate was set to  $10^{-3}$ , and we employed a learning rate decay strategy. Specifically, we decayed the learning rate by 50% every 100 epochs, which helped to prevent over-fitting and improve the generalization ability

of our model. We conducted our training on a NVIDIA RTX 3090 GPU.

The training process took approximately 25 minutes to complete. To ensure the robustness and reliability of our results, we employed a 5-fold cross-validation strategy. The 163 valid pairs of facial scans were shuffled and split into 5 consecutive folds. Each fold was used once as the validation set, while the remaining four folds formed the training set. Data splitting was performed prior to data augmentation, which was applied exclusively to the training dataset. We report the average score in Table 2.

### 4.3. Gallery

In our gallery, we present four patients with their real postoperative appearances alongside prediction results from our algorithm and the linear network using the Basel model. To assess accuracy, we also conducted texture transfer experiments on the Basel network, comparing it to LARS, the best model from [12]. Bimaxillary orthognathic surgery, with or without genioplasty, was performed for all four patients, shown in Fig. 3. For the first patient, our approach effectively predicted the outcome of mouth correction, with minor discrepancies in the lower face compared to LARS. In the lower nasal region, the linear model predicted a longer, wider, and lower nasal base, deviating from the surgical plan. For the second patient, our algorithm successfully predicted the jaw’s repositioning, while LARS did not resolve the protruding chin. For the third and fourth patients, both of whom had bimaxillary orthognathic surgery with genioplasty to shorten facial length by adjusting the chin’s tilt angle, our algorithm accurately predicted the jaw’s angle change, resulting in a more aesthetically pleasing facial shape. LARS, however, failed to predict these changes accurately.

### 4.4. ablation studies

We conducted an ablation study to examine the effectiveness of the four losses and data augmentation techniques introduced in our model. Both quantitative (as shown in Table. 1) and qualitative (as shown in Figure. 4) results demonstrate the efficacy of these techniques. Our findings suggest that the incorporation of these four losses and data augmentation can significantly improve the performance and efficacy of our model.

Table 1: Ablation study of our model

Prediction Network	Hausdorff Distance (mm)	Chamfer Distance (mm)	Training Data Amount
<b>OUR’s</b>	<b>8.999</b>	<b>2.503</b>	<b>1330</b>
- Mouth-convexity loss	9.009	2.561	1330
- Asymmetry loss	9.142	2.571	1330
- Latent code loss	9.047	2.635	1330
- Geometry loss	9.237	2.644	1330
- Augmentated Data	9.517	2.940	133

### 4.5. User study

The user experiment aimed to test whether participants could distinguish between machine learning-generated faces and real surgical outcomes. We collected pre- and post-surgery 3D data for each patient, parameterized with FLAME and transferred textures for consistency. To aid participants in observing facial symmetry and feature positioning, we provided frontal and side views, along with an animation rotating 180 degrees from left to right. Pre-operative data was clearly labeled, and participants had to identify if the real surgical outcome appeared before or after the machine-predicted result. Participants included five medical professionals (two surgeons, three orthodontists) and 15 engineers (12 males, 3 females). Using a 2 Alternative Forced Choice format and a t-test, results showed 49.3% of medical professionals and 50.2% of engineers chose our solution, with p-values of 0.84 and 0.88, respectively. This indicated neither group could distinguish between the two outcomes.

### 4.6. Quantitative comparison

We quantitatively compared the error of our prediction network with that of LARS, and found that our network outperformed LARS in both the Chamfer distance and Hausdorff distance metrics, as shown in Table 2. Additionally, we observed that data augmentation was very helpful in improving our performance, but had little effect on the performance of LARS.

### 4.7. application

We created an animation by interpolating the latent vectors, which can be used to show patients a transformation from pre-surgery to post-surgery, as shown in Fig. 5. This allows patients to visualize the movement of their chins and the change in their overall facial appearance. For a better demonstration, please refer to our supplementary video.

## 5. Conclusion

In this paper, we introduce a novel method for predicting facial appearance following orthognathic treatment using only 3D face geometry. During the training phase, our approach utilizes customized mouth-convexity and asymmetry losses, combined with latent code and geometric losses, to outperform existing methods in terms of accuracy. Our experimental results demonstrate significant potential for real-world clinical applications. Validating the method’s effectiveness in actual clinical settings is planned for our future research.

**Limitation.** Our current model doesn’t offer multi-modal predictions based on factors like age, gender, and skin condition due to the use of unlabeled data. However, with additional multi-modal labeled data in the future, we can categorize the existing data and make more targeted predictions without significantly reducing the

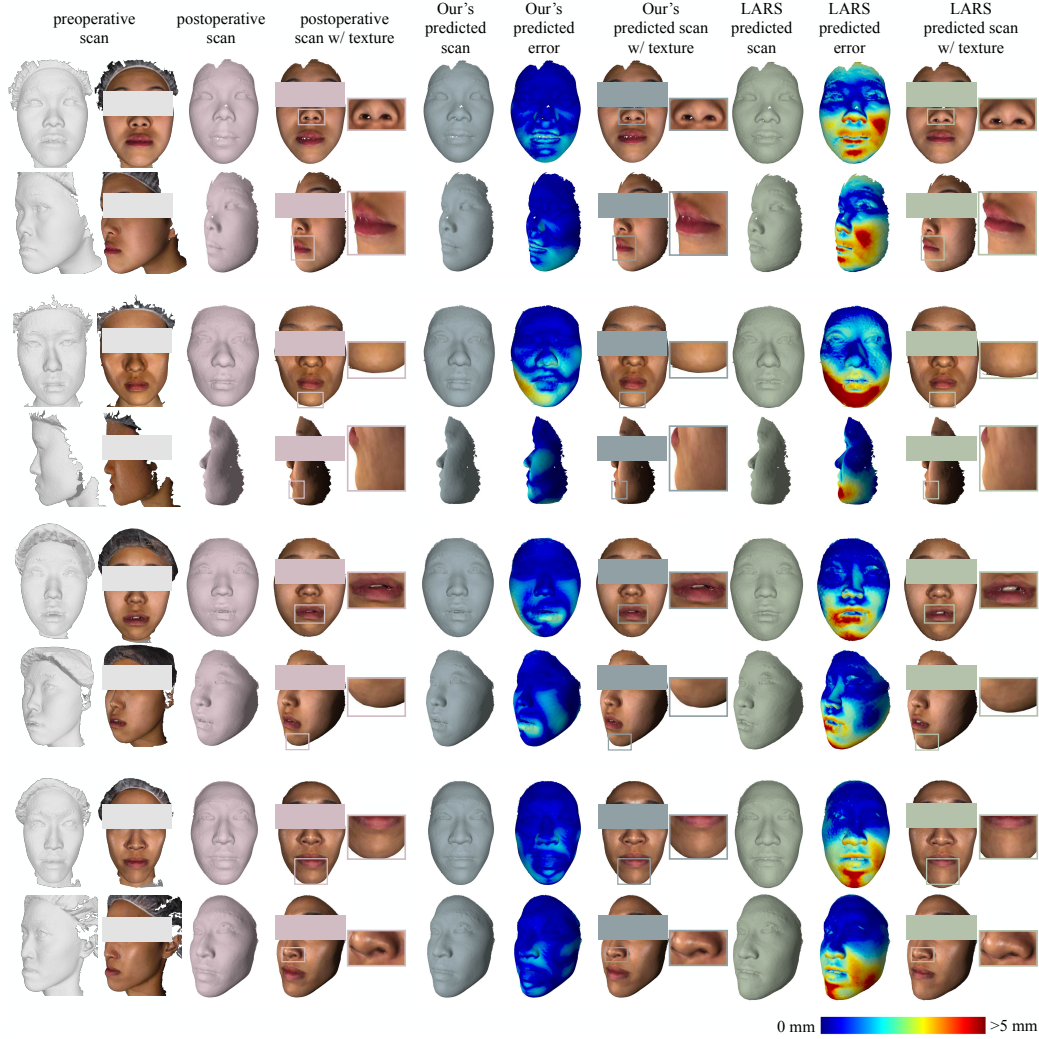


Figure 3: Comparison of our method with LARS across four patient cases. Ground truth (GT) pre- and post-surgical scans are shown on the left for reference. LARS predictions overestimated nose size and face length while underestimating lip thickness in the first, third, and fourth cases, and failed to adequately address the prominent chin in the second case. Our method effectively predicts surgical outcomes while preserving the patient’s natural appearance.

dataset. Our focus is on providing automatic visualizations for patients, not orthognathic professionals. In the future, we may add user-friendly interfaces with adjustable parameters for medical professionals if we develop a platform for surgical planning.

## References

- [1] 3dMD, 2022. 3dmd vultus. <http://www.4cmedikal.com.tr/>.
- [2] Booth, J., Roussos, A., Zafeiriou, S., Ponniah, A., Dunaway, D., 2016. A 3d morphable model learnt from 10,000 faces, in: Proceedings of the IEEE conference on computer vision and pattern recognition, pp. 5543–5552.
- [3] Chaiprasittikul, N., Thanathornwong, B., Pornprasertsuk-Damrongsri, S., Raocharernporn, S., Maponthong, S., Manopatanakul, S., 2023. Application of a multi-layer perceptron in preoperative screening for orthognathic surgery. *Healthcare Informatics Research* 29, 16–22.
- [4] Co., M., 2022. Morpheus3d for orthognathic surgical planning. <https://morpheus3d.co.kr/wp/en/clinical-services/orthognathic-surgical-planning-service/>.
- [5] Company, A.L., 2022. Modiface - augmented reality. <http://modiface.com/>.
- [6] Corp., P., 2022. Youcam. [tw.cyberlink.com/products/youcam](http://tw.cyberlink.com/products/youcam).
- [7] Corporation, S., 2022. B612. <https://b612.snow.me>.
- [8] Dobai, A., Markella, Z., Vízkelety, T., Fouquet, C., Rosta, A., Barabás, J., 2018. Landmark-based midsagittal plane analysis in patients with facial symmetry and asymmetry based on cbct analysis tomography. *Journal of Orofacial Orthopedics/Fortschritte der Kieferorthopädie* 79, 371–379.
- [9] Dong, X., Yu, S.I., Weng, X., Wei, S.E., Yang, Y., Sheikh, Y., 2018. Supervision-by-Registration: An unsupervised approach to improve the precision of facial landmark detectors, in: CVPR, pp. 360–368.
- [10] Elshebiny, T., Morcos, S., Mohammad, A., Quereshy, F., Valiathan, M., . Accuracy of three-dimensional soft tissue prediction in orthognathic cases using dolphin three-dimensional software. *Journal of Craniofacial Surgery* .
- [11] Jeong, S.H., Yun, J.P., Yeom, H.G., Lim, H.J., Lee, J., Kim, B.C., 2020. Deep learning based discrimination of soft tissue profiles requiring orthognathic surgery by facial photographs. *Scientific Reports* 10, 16235.
- [12] Knoops, P.G., Papaioannou, A., Borghi, A., Breakey, R.W., Wilson, A.T., Jeelani, O., Zafeiriou, S., Steinbacher, D., Padwa, B.L., Dunaway, D.J., et al., 2019. A machine learning frame-

Table 2: Performance Comparison

Algorithms	HD* (mm) ↓			CD* (mm) ↓			Data Amount
	mean	min	max	mean	min	max	
<b>OUR's</b>	<b>9.00</b>	<b>7.63</b>	<b>11.30</b>	<b>2.50</b>	<b>1.24</b>	<b>3.60</b>	<b>1330</b>
LARS	9.68	7.50	15.41	2.77	1.72	4.77	1330
OUR's w/o synthesized data	9.43	8.00	13.53	2.94	1.91	6.38	133
LARS w/o synthesized data	9.67	7.46	16.13	2.98	1.57	5.21	133

\* HD and CD represent Hausdorff and Chamfer Distance respectively.

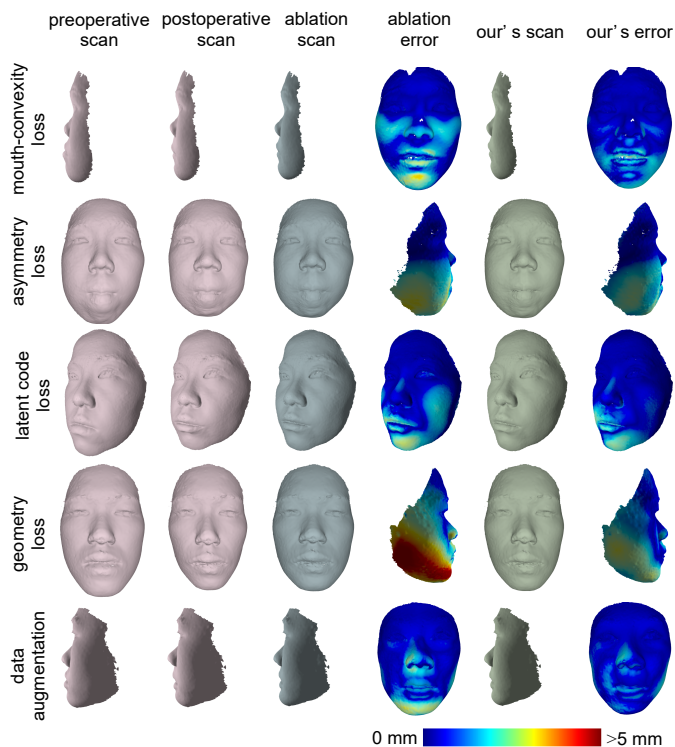


Figure 4: Removing the mouth-convexity loss leads to an overly prominent chin, while removal of the asymmetry loss results in facial asymmetry. Without the latent code loss, there is significant drift in the cheeks, and the overall error increases when the geometry loss is excluded. The addition of data augmentation can further reduce the prediction error.

work for automated diagnosis and computer-assisted planning in plastic and reconstructive surgery. *Scientific reports* 9, 1–12.

[13] Laurinavičius, D., Maskeliūnas, R., Damaševičius, R., 2023. Improvement of facial beauty prediction using artificial human faces generated by generative adversarial network. *Cognitive Computation* 15, 998–1015.

[14] Li, L., Bao, J., Yang, H., Chen, D., Wen, F., 2019. Faceshifter: Towards high fidelity and occlusion aware face swapping. *arXiv preprint arXiv:1912.13457*.

[15] Li, T., Bolkart, T., Black, M.J., Li, H., Romero, J., 2017. Learning a model of facial shape and expression from 4D scans. *ACM Proc. SIGGRAPH Asia* 36, 194:1–194:17.

[16] Liang, Y., Zhang, C., Zhao, J., Wang, W., Li, X., 2024. Skull-to-face: Anatomy-guided 3d facial reconstruction and editing.

[17] Ling, J., Wang, Z., Lu, M., Wang, Q., Qian, C., Xu, F., 2022. Structure-aware editable morphable model for 3d facial detail animation and manipulation, in: *Computer Vision–ECCV 2022: 17th European Conference, Tel Aviv, Israel, October 23–27, 2022, Proceedings, Part III*, Springer. pp. 249–267.

[18] Ma, L., Kim, D., Lian, C., Xiao, D., Kuang, T., Liu, Q., Lang, Y., Deng, H.H., Gateno, J., Wu, Y., et al., 2021. Deep simula-

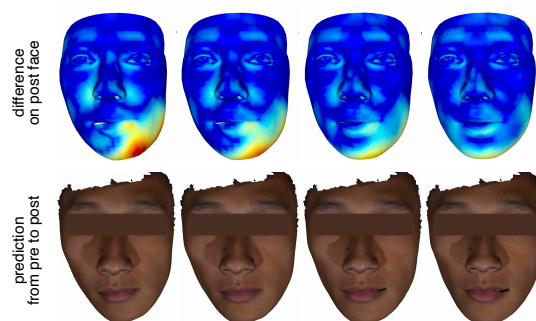


Figure 5: Visualization of the latent space interpolation results. The faces generated from interpolated latent codes are shown in the second row. The face on the far left is the pre-surgery face, and the face on the far right is the prediction of the post-surgery outcome. The first row represents the distances between these faces and the post-surgery face. Use the same color map as in Fig. 4.

tion of facial appearance changes following craniomaxillofacial bony movements in orthognathic surgical planning, in: *MIC-CAI*, Springer. pp. 459–468.

[19] Nirkin, Y., Keller, Y., Hassner, T., 2023. Fsganv2: Improved subject agnostic face swapping and reenactment. *IEEE T-PAMI* 45, 560–575.

[20] Park, J.A., Moon, J.H., Lee, J.M., Cho, S.J., Seo, B.M., Donatelli, R.E., Lee, S.J., 2024. Does artificial intelligence predict orthognathic surgical outcomes better than conventional linear regression methods? *The Angle Orthodontist*.

[21] Park, Y., Choi, J., Kim, Y., Choi, S., Lee, J., Kim, K., Chung, C., 2022. Deep learning-based prediction of the 3d postorthodontic facial changes. *Journal of Dental Research* 101, 1372–1379.

[22] Qiu, Z., Li, Y., He, D., Zhang, Q., Zhang, L., Zhang, Y., Wang, J., Xu, L., Wang, X., Zhang, Y., Yu, J., 2022. Sculptor: Skeleton-consistent face creation using a learned parametric generator 41.

[23] Saeed, J.N., Abdulazeez, A.M., Ibrahim, D.A., 2023. Automatic facial aesthetic prediction based on deep learning with loss ensembles. *Applied Sciences* 13, 9728.

[24] Steiner, C.C., 1960. The use of cephalometrics as an aid to planning and assessing orthodontic treatment: report of a case. *American journal of orthodontics* 46, 721–735.

[25] Tanikawa, C., Yamashiro, T., 2021. Development of novel artificial intelligence systems to predict facial morphology after orthognathic surgery and orthodontic treatment in japanese patients. *Scientific reports* 11, 1–11.

[26] Ter Horst, R., van Weert, H., Loonen, T., Bergé, S., Vinayahalingam, S., Baan, F., Maal, T., de Jong, G., Xi, T., 2021. Three-dimensional virtual planning in mandibular advancement surgery: Soft tissue prediction based on deep learning. *Journal of Cranio-Maxillofacial Surgery* 49, 775–782.

[27] Yoo, J.H., Yeom, H.G., Shin, W., Yun, J.P., Lee, J.H., Jeong, S.H., Lim, H.J., Lee, J., Kim, B.C., 2021. Deep learning based prediction of extraction difficulty for mandibular third molars. *Scientific Reports* 11, 1954.

[28] Yu, C., Wang, J., Peng, C., Gao, C., Yu, G., Sang, N., 2018.

Bisenet: Bilateral segmentation network for real-time semantic segmentation, in: ECCV, pp. 325–341.

- [29] Zhang, C., Bengio, S., Hardt, M., Recht, B., Vinyals, O., 2021. Understanding deep learning (still) requires rethinking generalization. *Communications of the ACM* 64, 107–115.
- [30] Zheng, W., Zhao, J., Liu, X., Pan, Y., Gan, Z., Han, H., Liu, N., 2023. Flame-based multi-view 3d face reconstruction, Springer-Verlag, Berlin, Heidelberg.